

# Estimates of Black Hole Spin Properties of 55 Sources

Ruth. A. Daly <sup>\*</sup>

*Penn State University, Berks Campus, Reading, PA 19608, USA*

7 March 2011

## ABSTRACT

Studies of black hole spin and other parameters as a function of redshift provide information about the physical state and merger and accretion histories of the systems. One way that black hole spin may be estimated is through observations of extended radio sources. These sources, powered by outflows from an AGN, allow the beam power and total outflow energy to be studied. In a broad class of models, the beam power of the outflow is related to the spin of the black hole. This relationship is used to estimate black hole spins for 55 radio sources. The samples studied include 7 FR II quasars and 19 FR II radio galaxies with redshifts between 0.056 and 1.79, and 29 radio sources associated with CD galaxies with redshifts between 0.0035 and 0.291. The FR II sources studied have estimated spin values of between about 0.2 and 1; there is a range of values at a given redshift, and the values tend to increase with increasing redshift. Results obtained for FR II quasars are very similar to those obtained for FR II galaxies. A broader range of spin values are obtained for the sample of radio sources associated with CD galaxies studied. The fraction of the spin energy extracted per outflow event is estimated and ranges from about 0.03 to 0.5 for FR II sources and 0.002 to about 1 for radio sources associated with CD galaxies; the data are consistent with this fraction being independent of redshift though the uncertainties are large. The results obtained are consistent with those predicted by numerical simulations that track the merger and accretion history of AGN, supporting the idea that, for AGN with powerful large-scale outflows, beam power is directly related to black hole spin.

**Key words:** black hole physics – galaxies: active

## 1 INTRODUCTION

Black hole spin and mass are the fundamental parameters that characterize a supermassive black hole. Black hole spin is related to the merger and accretion history of the black hole as discussed, for example, by Hughes & Blandford (2003), Volonteri et al. (2005), King & Pringle (2006, 2007), Volonteri, Sikora, and Lasota (2007), King, Pringle, & Hofmann (2008), and Berti & Volonteri (2008). Hughes & Blandford (2003) consider the coevolution of black hole mass and spin in binary merger scenarios and find that the holes are spun down by mergers. Volonteri et al. (2005) study the evolution of the full distribution of black hole spins in hierarchical galaxy formation theories including prolonged gas accretion and binary mergers. Volonteri, Sikora, and Lasota (2007) determine and compare spins of black holes in giant elliptical galaxies with those of disk galaxies and show that elliptical galaxies are likely to have higher spins on average than disk galaxies. King & Pringle (2006) suggest that accretion onto supermassive black holes occurs in a sequence

of randomly oriented accretion episodes. King & Pringle (2007) show that black hole growth that occurs in a series of small-scale randomly oriented accretion events leads to black hole spins that are less than one. King, Pringle, & Hofmann (2008) find that accretion of this type leads to supermassive black holes with moderate spin, and the spin value of an individual black holes may deviate significantly from the mean value. In addition, the mean spin value of the black hole population decreases slowly as black hole mass increases. Examples of holes with large spin parameter may occur and are most likely to be found in giant elliptical galaxies. Berti & Volonteri (2008) show that the redshift evolution of black hole spins for a given population of sources can be used to determine the merger and accretion history of the sources and whether the accretion is prolonged or occurs in short-lived chaotic events. Thus, studies of spin as a function of redshift may be used as a diagnostic of the accretion and merger histories of AGN.

Spins of individual black holes may be determined by studies quite close to the AGN, or by studies of outflows from the AGN. Each method of measuring black hole spin is model-dependent. Spins of three objects have been obtained

\* E-mail: rdaly@psu.edu

by studies quite close to the heart of the AGN from X-ray measurements. Spins obtained using X-ray measurements of AGN are  $0.60 \pm 0.07$  for Fairall 9 (Schmoll et al. 2009),  $0.6 \pm 0.2$  for AGN SWIFT J2127.4+5654 (Miniutti et al. 2009), and  $0.92 - 0.99$  for MCG-6-30-15 (Brenneman & Reynolds 2006; Reynolds & Fabian 2008). The use of extended radio sources to study black hole spin is discussed and applied to one radio galaxy by McNamara et al. (2009) and to 48 radio galaxies by Daly (2009a,b). Daly (2009a) presents a “model-independent” method of placing a lower bound on the black hole spin. The outflow energy is taken as a lower bound on the black hole spin energy, and this bound is combined with the black hole mass to obtain a lower bound on the black hole spin. Powerful radio galaxies were found to have remarkably similar minimum spin values with a weighted mean of  $0.12 \pm 0.01$ . McNamara et al. (2009) studied the radio galaxy MS0735.6+7421 in the context of the hybrid model of Meier (1999, 2001) and concluded that the outflow is likely powered by the spin energy of a maximally spinning hole. Daly (2009b) studied 48 extended radio galaxies with redshifts between zero and two, including MS0735.6+7421, in the context of the Meier (1999, 2001) and Blandford & Znajek (1977) models of spin energy extraction and obtained an estimate of the spin of each black hole assuming that the magnetic field strength is proportional to the black hole spin; the black hole spins obtained range from about 0.1 to 1. The results suggest that the black hole spin increases slowly with redshift over the redshift range from zero to two.

The work presented here on extended radio sources expands and improves upon prior studies, which included only radio galaxies, in several ways. A sample of 7 FR II quasars is included here, and spin estimates obtained with these sources are compared with results obtained with radio galaxies. In the prior study, a magnetic field strength  $B \propto j$  was considered. Here, two additional characterizations of the magnetic field are considered, and results obtained with different field strength characterizations are compared. In addition, the spin energy per unit black hole mass is obtained for the 7 FR II quasars, and a new quantity, the fraction of the spin energy extracted per outflow event is obtained and studied for 7 FR II quasars, 19 FR II galaxies, and 29 radio sources associated with CD galaxies.

The methods of estimating the black hole spin, the spin energy per unit black hole mass, and the fraction of spin energy extracted per outflow event are described in section 2, results are presented and discussed in section 3, and conclusions follow in section 4.

## 2 THE METHOD

Large-scale radio sources are powered by twin jets that emanate from the AGN. A class of models have been proposed and developed in which the jets are powered in part or in full by the spin energy associated with a rotating black hole and surrounding region (e.g. Blandford & Znajek 1977; Rees 1984; Begelman, Blandford, & Rees 1984; Punsly & Coroniti 1990; Blandford 1990; Meier 1999, 2001; Koide et al. 2000; McKinney & Gammie 2004; De Villiers et al. 2005; Hawley & Krolik 2006). In many of these models there is a relationship between the beam power (or energy per unit time)  $L_j$  carried by the jet, the black hole mass  $M$ , spin  $j$ ,

and “braking” magnetic field strength  $B$ , which takes the form  $L_j \propto B^2 M^2 j^2$  where  $j \equiv a/m$ ,  $a$  is defined in terms of the spin angular momentum  $S$ , the speed of light  $c$ , and the black hole mass  $M$ ,  $a \equiv S/(Mc)$ , and  $m \equiv GM/c^2$ . For example, this proportionality applies to the Blandford & Znajek (1977) model (the “BZ” model), the modified BZ model discussed by Reynolds, Garofalo, & Begelman (2006), and the hybrid model of Meier (1999, 2001).

Thus, if the beam power and black hole mass for a given AGN are known, the black hole spin may be studied for various magnetic field strengths (e.g. Blandford 1990, Daly 2009b):

$$j = \kappa (L_{44})^{0.5} B_4^{-1} M_8^{-1} \quad (1)$$

where  $L_{44}$  is the beam power in units of  $10^{44}$  erg/s,  $B_4$  is the poloidal component of the magnetic field that threads the accretion disk and ergosphere in units of  $10^4$  G, and  $M_8$  is the black hole mass in units of  $10^8 M_\odot$ . The constant of proportionality  $\kappa$  varies by a factor of a few for different models; for example, in the hybrid model of Meier (1999)  $\kappa \approx (1.05)^{-1/2}$ , while in the model of Blandford & Znajek (1977)  $\kappa \approx \sqrt{5}$ .

A source with no outflow can still have a significant spin, but only sources with outflows provide the information necessary to deduce the spin. For example, in the magnetic switch model of Meier (1999, 2001), the outflow only occurs when the magnetic field strength reaches a particular value.

The black hole spin  $j$  can be used to determine the black hole spin energy  $E_s$  in terms of the black hole mass  $M$  (e.g. Rees 1984):

$$E_s/Mc^2 = 1 - \left( \frac{1 + [1 - j^2]^{1/2}}{2} \right)^{1/2}. \quad (2)$$

The fraction  $f$  of the spin energy extracted during a particular outflow event may be empirically determined by taking the ratio of the outflow energy  $E_*$  to the spin energy:

$$f \equiv E_*/E_s. \quad (3)$$

Black hole spins, spin energy per unit black hole mass, and the fraction of the spin energy extracted during a particular outflow event are estimated here for sources with empirical determinations of beam power and black hole mass. To obtain these estimates, three different characterizations of the magnetic field strength are considered. For each characterization, the range and redshift evolution of black hole spin and fraction of spin energy extracted are studied.

The field strengths considered are an Eddington magnetic field strength, a constant magnetic field strength, and a magnetic field strength that is proportional to the black hole spin. These three field strengths are related to the black hole properties in different ways. Interestingly, the overall results and general trends obtained with each characterization are rather similar. The Eddington magnetic field strength is the field strength such that the energy density of the magnetic field is equal to that of a radiation field with an Eddington luminosity (e.g. Rees 1984; Dermer, Finke, & Menon 2008); in units of  $10^4$  G,  $B_{4,EDD} \simeq 6M_8^{-1/2}$ . This is the field strength that is expected for sources radiating at the Eddington luminosity. King (2010) argues that many AGN are likely to be radiating at this luminosity for much of their lives. To evaluate the impact of an assumed characterization of the magnetic field strength on the quantities studied

here, we also consider results obtained assuming a constant magnetic field strength. This possibility has been suggested and considered by several authors (e.g. Rees 1984; Punsly & Coroniti 1990; Blandford 1990) and, more recently, Piotrovich et al. (2010). A characteristic value of  $10^4 G$ , or  $B_4 = 1$ , is generally adopted, and is used here; the results obtained here can easily be scaled to any other constant value of the field strength. For comparison, a third characterization of the magnetic field strength is considered. If it is assumed that the fraction of the spin energy extracted per outflow event is constant, then observations of FR II radio galaxies indicate that the magnetic field strength is proportional to the black hole spin,  $B_4 \simeq 2.78j$  (Daly & Guerra 2002; Daly et al. 2009). Interestingly, this is also indicated by a comparison of the beam power predicted in the hybrid model of Meier (1999, 2001) and empirical results obtained by Allen et al. (2006) and Merloni & Heinz (2007). The results of Allen et al. (2006) and Merloni & Heinz (2007) indicate that the beam power is proportional to the accretion rate to the power 1.3 and 1.6, respectively, while equation (12) of Meier (1999) indicates that the beam power is proportional to the accretion rate to the power 1.6 when  $B \propto j$ . Thus, it is possible that the field strength is related to the black hole spin, and it is useful to consider this case as a comparison.

### 3 RESULTS

#### 3.1 The Samples

The method is applied to 7 powerful FR II quasars, 19 powerful FR II galaxies, and 29 central dominant (CD) galaxies, and includes most sources for which the black hole mass and beam power of the outflow have been empirically determined. The beam powers and black hole masses for the sources are illustrated in Fig. 1 and listed in Tables 1 and 2. The FR II quasars and galaxies have a similar range of beam power and the quasars have a slightly broader range of black hole mass than the galaxies. Most of the CD galaxies have substantially lower beam powers and extend to lower masses than the FR II sources; this is due to the fact that most of the CD sources are quite nearby and can be observed to relatively low flux levels.

The FR II quasars are obtained from the samples of Leahy, Muxlow, & Stephens (1989) and Liu, Pooley, & Riley (1992), and their properties including beam powers are summarized by Wellman, Daly, & Wan (1997) and Wan, Daly, & Guerra (2000). All quantities have been computed in a standard spatially flat cosmological model with current mean mass density  $\Omega_m = 0.3$ , cosmological constant  $\Omega_\Lambda = 0.7$ , and a value of Hubble's constant of  $H_0 = 70 \text{ km s}^{-1} \text{ kpc}^{-1}$ . The beam power  $L_j$  of the outflow is determined from the pressure of the forward region of the radio lobe, the lobe width, and the rate of growth of the extended lobes by applying the equations of strong shock physics. As noted by O'Dea et al. (2009), this determination of the beam power does not depend upon the offset of the plasma in the radio lobe from minimum energy conditions due to a chance cancellation of the way this offset enters the determination of the beam power. The total energy that will be expelled by the outflow over its entire lifetime,  $E_*$ , is obtained from the beam power using the relation established for powerful radio

galaxies  $E_* \propto L_j^{1/2}$  (O'Dea et al. 2009; Daly et al. 2009; Daly & Guerra 2002). Quantities are obtained for each side of a source, and the total value is taken to be twice the weighted mean of that for the two sides of the source.

The sample of 19 FR II radio galaxies is obtained from sources studied by Leahy, Muxlow, & Stephens (1989), Liu, Pooley, & Riley (1992), Guerra, Daly, & Wan (2000), and O'Dea et al. (2009). Their properties including beam powers are summarized by O'Dea et al. (2009), and are obtained in the same manner as described above for FR II quasars.

The black hole masses of the FR II quasars are obtained from McLure et al. (2006), those for the FR II radio galaxies are obtained from Tadhunter et al. (2003), McLure et al. (2004), and McLure et al. (2006), and those for the CD galaxies are obtained from the values  $M_{BH,LK}$  listed by Rafferty et al. (2006) after removing the correction factor of 0.35 to bring the black hole masses of Cygnus A and M84 into agreement with those of Tadhunter et al. (2003) and Maciejewski & Binney (2001).

The CD sample is obtained from Rafferty et al. (2006), and consists primarily of FRI sources (Fanaroff & Riley 1974). The total outflow energies  $E_*$  are estimated by Rafferty et al. (2006) from the pressure and volume of the cavity that is occupied by the radio emitting plasma, and the beam powers  $L_j$  are obtained by dividing the outflow energy by the buoyancy timescale  $t$ . The authors explain that this timescale is probably an overestimate of the true timescale, in which case the beam powers would increase, while the energy of the cavity could be due to multiple outflow events, which would cause the outflow energies and beam powers to decrease.

The source Cygnus A (3C 405) appears in both Table 1 and 2. The values listed in each table are obtained using independent methods. The beam power of  $(47 \pm 8) \times 10^{44}$  erg/s listed in Table 1 is obtained by applying the equations of strong shock physics to the forward region of the source (Wan, Daly, & Guerra 2000; modified to account for the different cosmological model adopted), while the value of  $(13 \pm 7) \times 10^{44}$  erg/s listed in Table 2 is obtained by dividing the energy required for the plasma to create and occupy the lobes by the buoyancy timescale (Rafferty et al. 2006); Rafferty et al. (2006) explain that the beam power obtained in this way may be an underestimate since the buoyancy timescale may be an overestimate. Given that there is only one source that is common to both methods, it is not possible to do a detailed comparison of the methods, and in order to compare results obtained with a given method, values obtained with that method are not modified. The black hole mass estimates for Cygnus A listed in Tables 1 and 2 are also obtained with two methods, and are in reasonably good agreement.

The FR II galaxies and quasars studied here are the most powerful FR II radio sources at their respective redshift, and the hosts have been identified as massive elliptical galaxies (e.g. Lilly & Longair 1984; Best, Longair, & Rottgering 1998; McLure et al. 2004). Thus, the powerful FR II and CD sources studied are likely to be drawn from the same parent population. Since the FR II sources represent the most powerful sources are their respective redshifts, they likely represent the envelope of the distribution, while the CD sample contains sources at low redshift with a very broad range of radio powers.

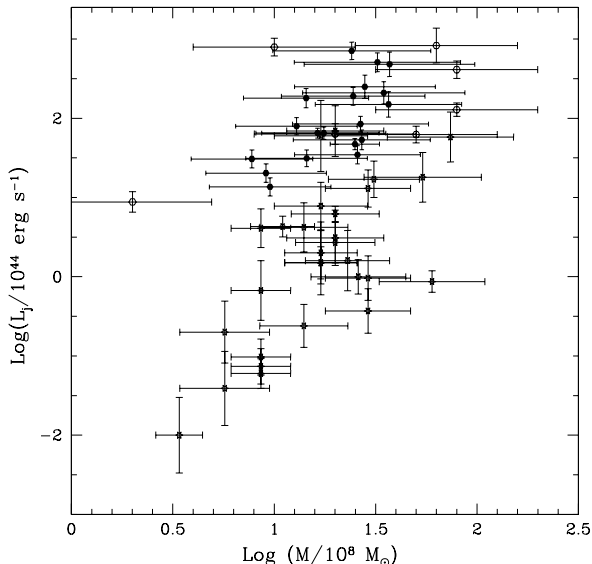


**Figure 1.** Beam powers and black hole masses for 55 AGN; FRII quasars are shown as open circles, FRII galaxies are shown as solid circles, and CD sources are shown as open stars.

The radio emitting regions of the sources studied are quite large (typically larger than the optical size of the host galaxy), and the timescale of the outflows are estimated to be millions to hundreds of millions of years (e.g. Rafferty et al. 2006; O’Dea et al. 2009). Thus, it is the very long term average properties of the outflows that are studied. The beam powers are obtained by applying the strong shock equations for FRII sources, and the pressure confinement equations for radio sources associated with CD galaxies in clusters of galaxies, so beam power determinations do not rely on an empirically or theoretically determined relationship between radio power and beam power. The sources are very large, with smoothly varying radio emission; the synchrotron radiation is not Doppler boosted or beamed, so there are no relativistic correction factors of this type. In addition, the overall rate of growth of the sources is not relativistic (e.g. O’Dea et al 2009; Rafferty et al. 2006). Thus, the use of the large extended radio emitting regions around AGN to determine the beam power is relatively simple and straight forward. In this sense, the AGN outflows studied here are quite different from those associated with X-ray binaries. Outflows from X-ray binaries can be highly variable on relatively short timescales, and can be strongly affected by Doppler boosting and beaming. The complex nature of outflows from X-ray binaries does not allow the direct application of physical principles to obtain the beam power of each outflow from detailed studies of that outflow; a theoretically motivated scaling between radio luminosity and beam power is used to obtain the beam power. The different source properties studied may make it difficult to compare results obtained with large extended radio sources to those obtained with X-ray binaries.

### 3.2 Determination of the Black Hole Spin

The black hole spin  $j$  depends upon the beam power, black hole mass, and magnetic field strength, and is determined for each of the three field strengths considered using equation (1) in the context of the Meier (1999, 2001) model, labeled  $j_M$ . Values of  $j_M$  and their uncertainties are listed in Tables 1 and 2, and are shown in Figures 2 - 7. To obtain the fractional uncertainty of  $j$ , the fractional uncertainties of the input parameters are combined in quadrature after noting the following. When  $B = B_{EDD}$ , we have that  $j \propto \sqrt{(L_{44}/M_8)}$  (so the fractional uncertainty of  $j$  is rather small). When  $B$  is constant, the fractional uncertainty of  $j$  is larger since  $j \propto \sqrt{L_{44}}M_8^{-1}$ . When  $B \propto j$ ,  $j \propto (L_{44})^{1/4}M_8^{-1/2}$ , so the fractional uncertainty of  $j$  is quite small.

For all three magnetic field strengths, the black hole spin increases with increasing redshift. Fits are obtained using the FRII galaxies and quasars only. The FRII sources are from the complete 3CR survey (Bennett 1962) including sources from the sample subsets of Laing, Riley, & Longair (1983) and Pooley et al. (1987); the selection effects for the sample are well understood. As mentioned above, the FRII sources studied are the most powerful sources at their respective redshifts and define the envelope of the distribution of sources.

The slope of  $\text{Log}(j_M)$  as a function of  $\text{Log}(1+z)$  is  $1.1 \pm 0.2$  for  $B = B_{EDD}$ ;  $0.86 \pm 0.36$  for  $B = 10^4$  G; and  $0.43 \pm 0.18$  for  $B \propto j$ , and are shown in Figures 2-4. These slopes are independent of the value of  $\kappa$  and thus are valid for a broad range of models. In all cases, the black hole spin is increasing with redshift. The reduced  $\chi^2$ s of the fits are less than one suggesting that the fits may be a bit more significant than indicated above. The quasars and radio galaxies have a similar range of black hole spin at a given redshift, and similar trend with redshift. For the field strengths considered, the FRII sources have spins that range from about 0.2 to 1, and, as noted above, there is a consistent trend of spin increasing with increasing redshift. The FRII sources are the most powerful sources at their respective redshifts and thus are likely to define the envelope of the source distribution. The black hole spins associated with the CD galaxies studied range from about  $10^{-2}$  to about 0.4.

Figs. 5, 6, and 7 show the black hole spin as a function of black hole mass for the three magnetic field strengths considered. The FRII galaxies have a small range of black hole mass relative to FRII quasars, and no dependence of spin on black hole mass is evident for the radio galaxies. The FRII quasars have a broader range of black hole mass than the radio galaxies, and the quasar sample is lacking sources with masses that overlap those of the galaxies, so it would be valuable to acquire and study quasars with black hole masses in this range. The CD galaxies have a range of black hole mass that is similar to the FRII galaxy and quasar sample, and a much broader range of spin, with spins extending to very low values. This is likely due to the way that the CD sample is selected.

Note that in the magnetic switch model of Meier (1999, 2001), outflows are only produced when the magnetic switch is activated. Sources with no outflows can have large spin values; spin values can only be deduced for sources with outflows.

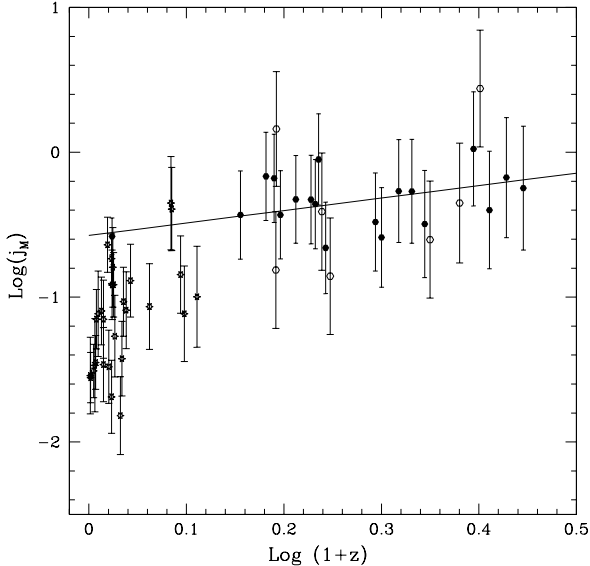


**Figure 2.** Black hole spins obtained with a constant magnetic field strength of  $10^4$  G; the symbols are as in Fig. 1. The line is the best fit to the FRII radio galaxies and quasars only and has a slope of  $0.86 \pm 0.36$  and a  $\chi^2$  of 13.28 for 24 degrees of freedom.

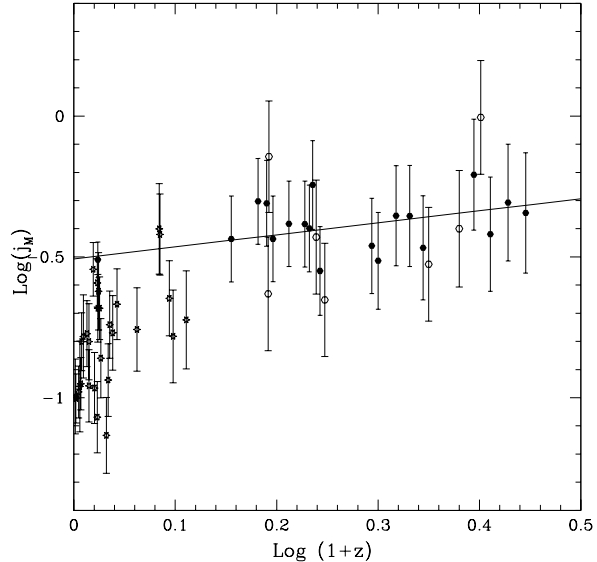


**Figure 4.** Black hole spin obtained with a magnetic field strength that is proportional to the spin; the symbols are as in Fig. 1. The line is best fit to the FRII radio galaxies and quasars and has a slope of  $0.43 \pm 0.18$  and a  $\chi^2$  of 13.2 for 24 degrees of freedom.

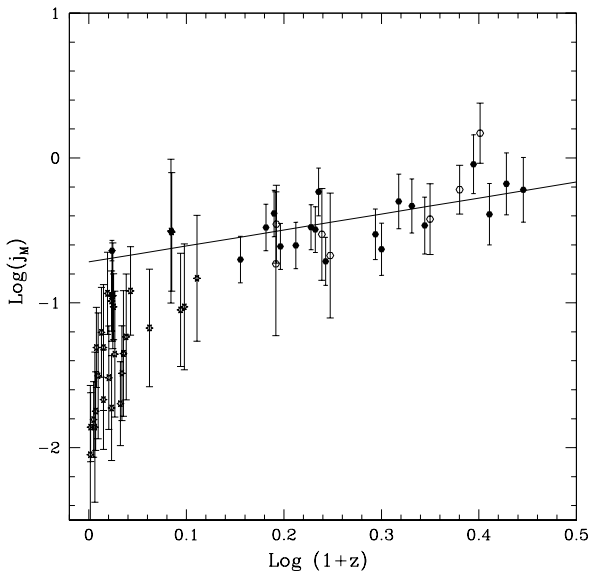


**Figure 3.** Black hole spins obtained with an Eddington magnetic field strength; the symbols are as in Fig. 1. The line is best fit to the FRII radio galaxies and quasars and has a slope of  $1.1 \pm 0.2$  and a  $\chi^2$  of 18.0 for 24 degrees of freedom.

### 3.3 Determination of the Spin Energy and the Fraction of Spin Energy Extracted

After the spin  $j$  has been determined, the spin energy  $E_s$  can be obtained using equation (2), and the fraction of the spin energy extracted during a particular outflow event can be obtained using equation (3). The spin energy  $E_s$  depends upon the spin  $j$  and the black hole mass  $M$ , while the fraction of the spin energy extracted  $f$  depends on these quan-

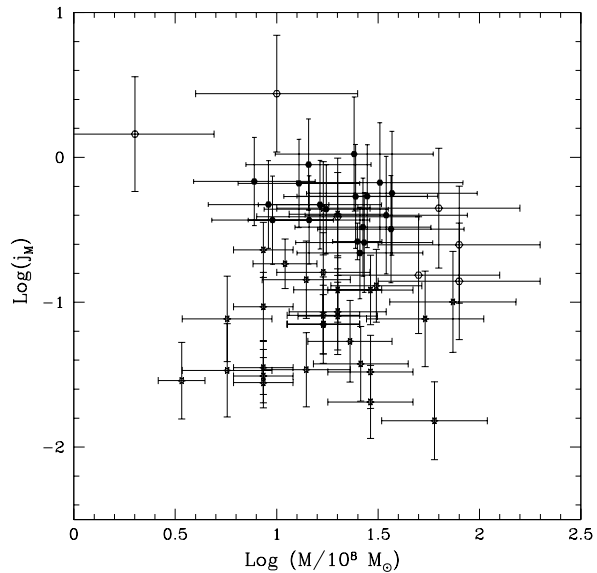


**Figure 5.** As in Fig. 2 but for spin as a function of black hole mass.

tities and the total outflow energy  $E_*$ . When  $j$  is greater than unity,  $E_s$  and  $f$  can not be determined (e.g. 3C437, 3C270.1 and 3C275.1). The values of  $E_s/(Mc^2)$ ,  $f$ , as well as  $E_*/(Mc^2)$  are listed in Tables 3 and 4, and  $f$  as a function of redshift is shown in Figs. 8 and 9. Only two magnetic field strengths,  $B = B_{EDD}$  and  $B_4 = 1$ , are considered here; the conclusion that  $B \propto j$  was obtained by assuming that  $E_* \propto E_s$  (or  $f$  is constant), as described in section 2, so  $f$  is, by construction, constant in that case.

The values of  $E_s/(Mc^2)$  obtained are all much less than

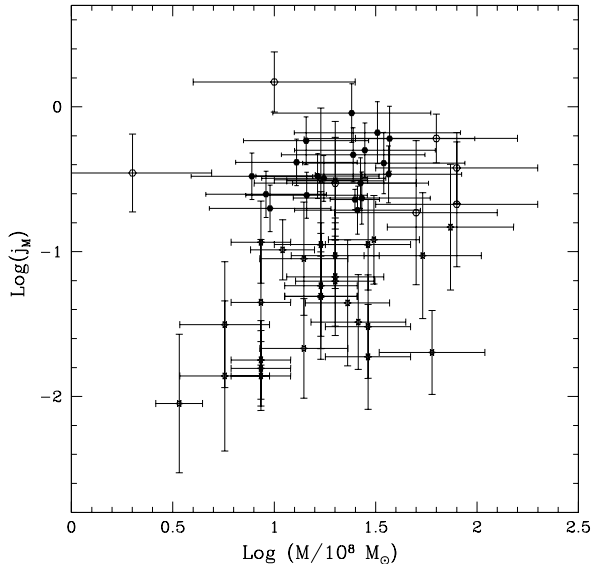


**Figure 6.** As in Fig. 3 but for spin as a function of black hole mass.

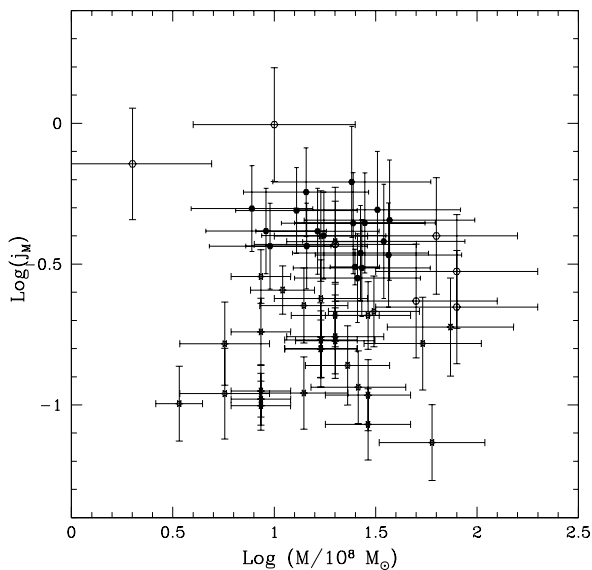


**Figure 7.** As in Fig. 4 but for spin as a function of black hole mass.

1. This occurs because  $r \equiv E_s/(Mc^2)$  is a very steep function of  $j$ , ranging from a value of  $r \approx 10^{-3}$  for  $j = 0.1$  to a maximum value of  $r \approx 0.29$  for  $j = 1$  (e.g. Rees 1984; Blandford 1990), so  $r$  is generally small. Equation (2) can be re-arranged to write the black hole spin  $j$  in terms of the spin energy per unit black hole mass  $r \equiv E_s/(Mc^2)$ :  $j = 2(2r - 5r^2 + 4r^3 - r^4)^{1/2}$ . Note that by replacing the spin energy  $E_s$  with the outflow energy  $E_*$ , this expression may be used to obtain a lower bound on the black hole spin that depends only upon the outflow energy and black hole mass (Daly 2009a).

The fraction of the spin energy extracted per outflow

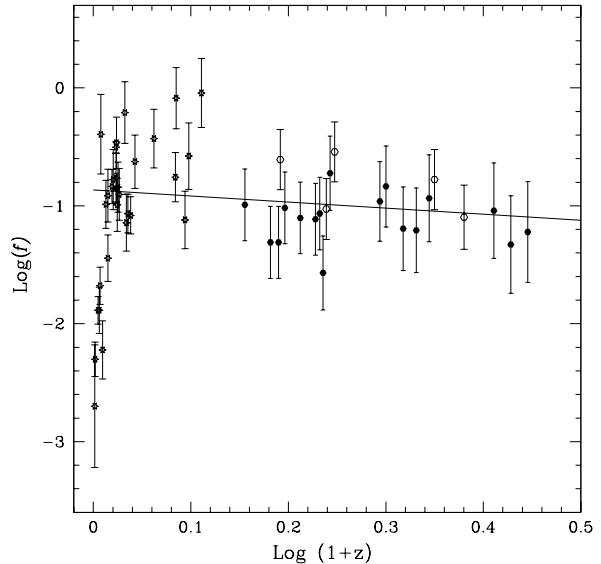


**Figure 8.** Fraction of the spin energy extracted as a function of redshift for  $B = 10^4$  G; the symbols are as in Fig. 1. The best fit line to the FRII radio galaxies and quasars is shown and has a slope of  $-0.52 \pm 0.41$  and a  $\chi^2$  of 14.8 for 21 degrees of freedom. This is consistent with no evolution of  $f(z)$ .

event  $f$  has a smaller range for the FRII sources studied than for the CD galaxies studied. The range of  $f$  for FRII sources is about 0.04 to 0.5 for  $B = B_{EDD}$  and 0.03 to 0.3 for  $B = 10^4$  G, and FRII quasars have values very similar to FRII galaxies. The range of  $f$  for CD galaxies is about 0.02 to greater than 1 for  $B = B_{EDD}$  and 0.002 to 0.9 for  $B = 10^4$  G. The values of  $f$  for the CD galaxies may be uncertain since this quantity depends primarily upon the buoyancy timescale for CD galaxies and, as discussed by Rafferty et al. (2006), this is likely to be an upper limit (see also the discussion in section 3.1).

The redshift evolution of  $f$  is studied using the FRII sources only, and is illustrated in Figs. 8 and 9. For  $B = 10^4$  G, the best fit slope of  $\text{Log}(f)$  as a function of  $\text{Log}(1+z)$  is  $-0.52 \pm 0.41$  with a  $\chi^2$  of 15 for 21 degrees of freedom. This is consistent with no evolution of  $f$  with  $z$ . The values of  $f$  and redshift evolution of FRII quasars is consistent with that of FRII galaxies, though the number of quasars is small and more data will be needed to confirm this. For  $B = B_{EDD}$ , the best fit slope is  $-1.8 \pm 0.4$  with a  $\chi^2$  of 276 for 23 degrees of freedom. The  $\chi^2$  is quite large; to bring the reduced  $\chi^2$  to unity would require increasing the uncertainty per point by a factor of about 3.5, which would change the uncertainty of the best fit slope to  $-1.8 \pm 1.3$ , consistent with no evolution. Thus, the data are consistent with no redshift evolution of  $f$  with redshift with a slight hint that  $f$  may decrease with increasing redshift. As mentioned earlier,  $B \propto j$  was obtained by assuming that  $f$  is constant (Daly & Guerra 2002; Daly et al. 2009).

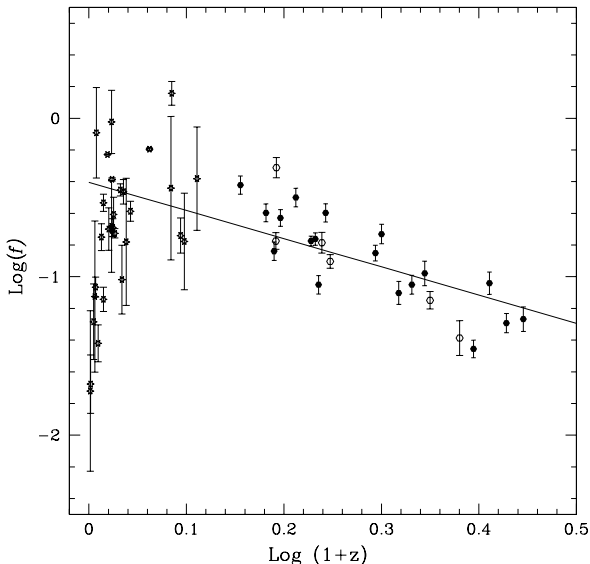


**Figure 9.** Fraction of the spin energy extracted as a function of redshift for  $B = B_{EDD}$ ; the symbols are as in Fig. 1. The best fit line to the FR II radio galaxies and quasars is shown and has a slope of  $-1.78 \pm 0.37$  and a  $\chi^2$  of 276 for 23 degrees of freedom. To bring the reduced  $\chi^2$  to unity would require increasing the uncertainty per point by about 3.5, which would change the uncertainty of the best fit slope to  $-1.8 \pm 1.3$ , so these data do not require that  $f(z)$  be strongly evolving with redshift.

#### 4 SUMMARY AND CONCLUSION

Black hole spins are estimated for extended radio sources fed by outflows from AGN assuming that the beam power of the outflow is related to the spin energy of the black hole and surrounding region. Samples of 7 powerful radio loud quasars, 19 powerful radio galaxies, and 29 CD galaxies with redshifts between about zero and two are studied. All of the sources are likely to be associated with massive elliptical galaxies. The black hole spins obtained for powerful FR II quasars and galaxies range from about 0.2 to 1 and are largest at high redshift and systematically decrease to lower redshift. This is the case for each of the three characterizations of the magnetic field strength considered. The powerful radio galaxies and quasars are drawn from the 3CR sample and are the most powerful sources at their respective redshifts; results obtained with these sources are likely to represent the envelope of the distribution. The spins of the radio sources associated with CD galaxies range from about 0.01 to 0.4. The CD sources are a heterogeneous sample and include many nearby low luminosity radio sources.

The normalization of the black hole spin,  $\kappa$ , varies by factors of a few for different specific models of spin energy extraction from the hole, ergosphere, and surrounding region. The trend of black hole spin increasing with redshift indicated by the analysis presented here is independent of the value of  $\kappa$ ; different values of  $\kappa$  will modify the overall normalization of the spins values, changing all of the spins by the same factor. If independent spin determinations of one or more of these sources are obtained, the value of  $\kappa$  could be empirically constrained or determined.

The decrease of the black hole spin with decreasing

redshift is consistent with the predictions of the models of Hughes & Blandford (2003) and King, Pringle, & Hofmann (2008). This suggests that beam power is directly related to black hole spin. Given the indications of the evolution of spin with redshift for massive elliptical galaxies obtained here, detailed models for the accretion and merger history of the sources and the type of accretion that occurs can be constructed, as discussed by Berti & Volonteri (2008). Clearly, the results presented here are along the lines of the predictions of King, Pringle, & Hofmann (2008) in that the mean spin decreases monotonically with decreasing redshift, source to source spins have fluctuations of order 0.2, and the spin tends to decrease with increasing black hole mass for the homogeneous sample of 3CR sources (though this is rather tentative because the black hole mass is an input to the spin determination). Consistency between model predictions and the estimated spins suggests that the beam power is directly related to black hole spin.

The fraction of the spin energy extracted per outflow event ranges from about 0.03 to 0.5 for FR II quasars and galaxies, and from about 0.002 to about one for radio sources associated with CD galaxies. The results are consistent with this fraction being independent of redshift. When this fraction is high, the outflow can significantly modify the spin of the hole, while when this fraction is low, the outflow has a small effect on the black hole spin. In this case, the merger and accretion history of AGN will have a larger impact on black hole spin evolution than the outflow history.

The results obtained here may be considered in light of the work of Elvis, Risaliti, & Zamorani (2002), who find that black holes associated with AGN that produce the X-ray background must be rapidly spinning, on average, at the time that background is produced. Models developed by Gilli, Salvati, & Hasinger (2001) suggest that the X-ray background is produced by sources with a range of redshift with much of the background produced by sources with redshift between 1 and 3. The elliptical galaxies studied here are found to have high spins at redshift of about 2, with spins slowly decreasing to lower redshift. If the sources that produce the X-ray background have spins that evolve in a manner similar to those studied here, the results of Elvis, Risaliti, & Zamorani (2002) might suggest that the most mild evolution of spin with redshift is favored; in the context of the current study, this would favor the magnetic field strength  $B \propto j$ , which yields spins that evolve as  $(1+z)^{0.43 \pm 0.18}$ . Note that this field strength is also favored by a comparison of the empirical results of Allen et al. (2006) and Merloni & Heinz (2007) with spin energy extraction models, as described at the end of section 2. Another factor that would affect the production of the X-ray background is the normalization of the spin, through the factor  $\kappa$ . If the sources that produce the X-ray background have spins similar to those studied here, it would suggest a value of  $\kappa \simeq \sqrt{5}$  as indicated by the BZ model. In this case, the spins of FR II sources vary from values of order unity at a redshift of about 2 to about 0.7 at a redshift of about 0 (e.g. Daly 2009b). Given the range of redshift of sources contributing to the X-ray background, and the indications from this study that there is a range of spin values at a given redshift for radio sources, a detailed study would have to be carried out to determine whether the sources that produce the X-ray background could have

spin normalizations and redshift evolution similar to those obtained here for radio sources.

The spin values obtained here for AGN are in good agreement with typical spin values reported for X-ray binary systems, which are summarized by Fender et al. (2010). Studies of X-ray binaries have not indicated a link between black hole spin and the properties of the jets (Steiner et al. 2010; Fender et al. 2010; Gou et al. 2010), except for a correlation between the transient jet normalization and spin (Fender et al. 2010). According to Fender et al. (2010), the lack of a relationship between jet properties and spin for X-ray binaries could be due to a problem with the jet properties or speed determinations; a problem with the spin measurements; or a real lack of dependence of jet properties on spin. Studies of AGN suggest a link between the beam power of large-scale outflows and black hole spin (Sikora, Stawarz, & Lasota 2007). To date, the samples studied are rather small, and very different parts of the systems are used to study the jet properties of X-ray binaries and the beam powers of AGN, as described in section 3.1. Thus, it is not clear how significant the differences are between the relationship of beam power and spin for AGN and the relationship of jet properties and spin for X-ray binaries. If differences truly exist, it might suggest that more than one mechanism may lead to the formation of jets from the vicinity of a black hole. In related work, Fernandes et al. (2010) studied powerful radio galaxies, concluding that the accreted energy is channeled into jets with maximum efficiency for the most powerful sources, and suggesting that black hole spin plays a dominant role in the production of jets. Punsly (2010) compared jet efficiencies with currently popular “no net flux” models of spin energy extraction and found that these models could not account for the empirically determined jet efficiencies. The detailed study of Kovacs, Gergely, & Biermann (2010) suggests that efficient jets can be produced in the context of the BZ model of spin energy extraction.

Overall, the results obtained with powerful 3CR quasars are consistent with those obtained with 3CR galaxies. The sample of quasars studied is small and larger samples of quasars are needed to quantify this result. The quasar sample studied has a black hole mass range that is larger than that of the 3CR galaxies studied and a dearth of black hole masses that overlap those of the galaxies. There is a hint that the quasars may lie at the edges of the distribution of spins for 3CR sources at a given redshift, and this might be related to black hole mass. This can be tested with larger quasar samples, and with samples of powerful radio galaxies with a broader range of black hole mass.

## ACKNOWLEDGMENTS

It is a pleasure to thank Laura Brenneman, Kris Beckwith, Preeti Kharb, Brian McNamara, Chris Reynolds, and Chris O’Dea for interesting and helpful discussions of this work. I would also like to thank the referee and editor for helpful comments and suggestions.

## REFERENCES

- Allen, S. W., Dunn, R. J. H., Fabian, A. C., Taylor, G. B., & Reynolds, C. S. 2006, *MNRAS*, 372, 21
- Begelman, M. C., Blandford, R. D., & Rees, M. J. 1984, *Rev. Mod. Phys.* 56, 255
- Bennett, A. S. 1962, *MNRAS*, 68, 163
- Berti, E., & Volonteri, M. 2008, *ApJ*, 684, 822
- Best, P. N., Longair, M. S., & Rottgering, H. J. A. 1998, *MNRAS*, 295, 549
- Birzan, L., McNamara, B. R., Nulsen, P. E. J., Carilli, C. L., & Wise, N. W. 2008, *ApJ*, 686, 859
- Blandford, R. D. 1990, in *Active Galactic Nuclei*, ed. T. J. L. Courvoisier & M. Mayor (Berlin: Springer), 161
- Blandford, R. D., & Payne, D. G. 1982, *MNRAS*, 199, 883
- Blandford, R. D., & Znajek, R. L. 1977, *MNRAS*, 179, 433
- Brenneman, L. W., & Reynolds, C. S. 2006, *ApJ*, 652, 1028
- Daly, R. A. 2009a, *ApJL*, 691, L72
- Daly, R. A. 2009b, *ApJL*, 696, L32
- Daly, R. A., & Guerra, E. J. 2002, *AJ*, 124, 1831
- Daly, R. A., Mory, M. P., O’Dea, C. P., Kharb, P., Baum, S., Guerra, E. J., & Djorgovski, S. G. 2009, *ApJ*, 691, 1058-1067.
- Dermer, C. D., Finke, J. D., & Menon, G. 2008, *Proceedings of Science*, in press (arXiv:0810.1055)
- De Villiers, J. P., Hawley, J. F., Krolik, J. H., Hirose, S. 2005, *ApJ*, 620, 878
- Elvis, M., Risaliti, G., & Zamorani, G. 2002, *ApJ*, 565, L75
- Fanaroff, B. L., & Riley, J. M. 1974, *MNRAS*, 164, 31
- Fender, R. P., Gallo, E., & Russell, D. 2010, *MNRAS*, 406, 1425
- Fernandes, C. A. C., Jarvis, M. J., Rawlings, S., Martinez-Sansigre, A., Hatziminaoglou, E., Lacy, M., Page, M. J., Stevens, J. A., & Vardoulaki, E. 2010, *MNRAS*, in press
- Gilli, R., Salvati, M., & Hasinger, G. 2001, *A&A*, 366, 407
- Gou, L., McClintock, J. E., Steiner, J. F., Narayan, R., Cantrell, A. G., Bailyn, C. D., & Orosz, J. A. 2010, *ApJ*, 718, L122
- Guerra, E. J., Daly, R. A., & Wan, L. 2000, *ApJ*, 544, 659
- Hawley, J. F., & Krolik, J. H. 2006, *ApJ*, 641, 103
- Hughes, S. A., & Blandford, R. D. 2003, *ApJ*, 585, L101
- King, A. R. 2010, *MNRAS*, 408, 95
- King, A. R., & Pringle, J. E. 2006, *MNRAS*, 373, L90
- King, A. R., & Pringle, J. E. 2007, *MNRAS*, 377, L25
- King, A. R., Pringle, J. E., & Hofmann, J. A. 2008, *MNRAS*, 385, 1621
- Koide, S., Meier, D. L., Shibata, K., Kudoh, T. 2000, *ApJ*, 536, 668
- Kovacs, Z., Gergely, L. A., Biermann, P. L. 2010, arXiv:1007.4279
- Laing, R. A., Riley, J. M., & Longair, M. S. 1983, *MNRAS*, 204, 151
- Leahy, J. P., Muxlow, T. W. B., & Stephens, P. W. 1989, *MNRAS*, 239, 401
- Lilly, S. J., & Longair, M. S. 1984, *MNRAS*, 211, 833
- Liu, R., Pooley, G., & Riley, J. M. 1992, *MNRAS*, 257, 545
- aciejewski, F., & Binney, J. 2001, *MNRAS*, 323, 831
- McKinney, J. C., & Gammie, C. F. 2004, *ApJ*, 611, 977
- McLure, R. J., Jarvis, M. J., Targett, T. A., Dunlop, J. S., & Best, P. N. 2006, *MNRAS*, 368, 1395
- McLure, R. J., Willott, C. J., Jarvis, M. J., Rawlings, S., Hill, G. J., Mitchell, E., Dunlop, J. S., & Wold, M. 2004, *MNRAS*, 351, 347
- McNamara, B. R., Kazemzadeh, F., Rafferty, D. A., Birzan, L., Nulsen, P. E. J., Kirkpatrick, C. C., & Wise, M. W. 2009, *ApJ*, 698, 594
- Merloni, A., & Heinz, S. 2007, *MNRAS*, 381, 589
- Meier, D. L. 1999, *ApJ*, 522, 753
- Meier, D. L. 2001, *ApJ*, 548, L9
- Miniutti, G., Panessa, F., de Rosa, A., Fabian, A. C., Malizia, A., Molina, M., Miller, J. M., & Vaughan, S. M. 2009, *MNRAS*, 398, 255

- O'Dea, C. P., Daly, R. A., Kharb, P., Freeman, K. A., & Baum, S. 2009, *A&A*, 494, 471
- Piotrovich, M. Yu., Silant'ev, N. A., Gnedin, Yu. N., & Natsvlshvili, T. M. 2010, arXiv:1002.4948
- Pooley, G. G., Leahy, J. P., Shakeshaft, J. R., & Riley, J. M. 1987, *MNRAS*, 224, 847
- Punsly, B. 2010, arXiv:1012.1910
- Punsly, B., & Coroniti, F. V. 1990, *ApJ*, 354, 583
- Rafferty, D. A., McNamara, B. R., Nulsen, P. E. J., & Wise, M. W. 2006, *ApJ*, 652, 216
- Rees, M. 1984, *ARA&A*, 22, 471
- Reynolds, C. S., & Fabian, A. 2008, *ApJ*, 675, 1048
- Reynolds, C. S., Garofalo, D., & Begelman, M. C. 2006, *ApJ*, 651, 1023
- Schmoll, S., Miller, J. M., Volonteri, M., Cackett, E., Reynolds, C. S., Fabian, A. C., Brenneman, L. W., Miniutti, G., & Gallo, F. C. 2009, *ApJ*, 703, 2171
- Sikora, M., Stawarz, L., & Lasota, J. 2007, *ApJ*, 658, 815
- Steiner, J. F., Reis, R. C., McClintock, J. E., Narayan, R., Remillard, R. A., Orosz, J. A., Gou, L., Fabian, A., & Torres, M. A. P. 2010, arXiv:1010.1013
- Tadhunter, C., Marconi, A., Axon, D., Wills, K., Robinson, T. G., & Jackson, N. 2003, *MNRAS*, 342, 861
- Volonteri, M., Madau, P., Quataert, E., & Rees, M. J. 2005, *ApJ*, 620, 69
- Volonteri, M., Sikora, M., & Lasota, J.P. 2007, *ApJ*, 667, 704
- Wan, L., Daly, R. A., & Guerra, E. J. 2000, *ApJ*, 544, 671
- Wellman, G. F., Daly, R. A., & Wan, L. 1997, *ApJ*, 480, 79

**Table 1.** Black Hole Spins of FRII Sources

Source (1)	type (2)	$z$ (3)	$L_{44}^a$ (4)	$M_8^b$ (5)	$B_{EDD,A}$ (6)	$j_M(B = B_{EDD})$ (7)	$j_M(B = 10^4 G)$ (8)	$j_M(B \propto j)$ (9)
3C 405	RG	0.056	$47 \pm 8$	$25 \pm 7$	$1.2 \pm 0.2$	$0.23 \pm 0.04$	$0.27 \pm 0.08$	$0.31 \pm 0.05$
3C 244.1	RG	0.43	$14 \pm 4$	$9.5 \pm 6.6$	$1.9 \pm 0.7$	$0.20 \pm 0.07$	$0.38 \pm 0.26$	$0.37 \pm 0.13$
3C 172	RG	0.519	$31 \pm 8$	$7.8 \pm 5.4$	$2.2 \pm 0.7$	$0.33 \pm 0.12$	$0.70 \pm 0.49$	$0.50 \pm 0.17$
3C 330	RG	0.549	$80 \pm 20$	$13 \pm 9$	$1.7 \pm 0.6$	$0.41 \pm 0.15$	$0.68 \pm 0.47$	$0.49 \pm 0.17$
3C 427.1	RG	0.572	$31 \pm 8$	$14 \pm 10$	$1.6 \pm 0.5$	$0.25 \pm 0.09$	$0.38 \pm 0.26$	$0.37 \pm 0.13$
3C 337	RG	0.63	$20 \pm 6$	$9.1 \pm 6.2$	$2.0 \pm 0.7$	$0.25 \pm 0.09$	$0.48 \pm 0.34$	$0.41 \pm 0.14$
3C34	RG	0.69	$65 \pm 9$	$16 \pm 11$	$1.5 \pm 0.5$	$0.33 \pm 0.12$	$0.48 \pm 0.34$	$0.41 \pm 0.15$
3C441	RG	0.707	$65 \pm 12$	$18 \pm 12$	$1.4 \pm 0.5$	$0.32 \pm 0.12$	$0.45 \pm 0.32$	$0.40 \pm 0.14$
3C 55	RG	0.72	$180 \pm 50$	$14 \pm 10$	$1.6 \pm 0.6$	$0.58 \pm 0.22$	$0.91 \pm 0.66$	$0.57 \pm 0.21$
3C 247	RG	0.749	$35 \pm 9$	$26 \pm 18$	$1.2 \pm 0.4$	$0.19 \pm 0.07$	$0.22 \pm 0.16$	$0.28 \pm 0.10$
3C 289	RG	0.967	$85 \pm 19$	$27 \pm 21$	$1.2 \pm 0.4$	$0.30 \pm 0.12$	$0.34 \pm 0.26$	$0.35 \pm 0.13$
3C 280	RG	0.996	$53 \pm 15$	$27 \pm 21$	$1.2 \pm 0.4$	$0.23 \pm 0.1$	$0.26 \pm 0.21$	$0.31 \pm 0.12$
3C 356	RG	1.079	$250 \pm 85$	$28 \pm 22$	$1.1 \pm 0.5$	$0.50 \pm 0.22$	$0.55 \pm 0.45$	$0.44 \pm 0.18$
3C 267	RG	1.144	$190 \pm 50$	$24 \pm 20$	$1.2 \pm 0.5$	$0.47 \pm 0.2$	$0.55 \pm 0.45$	$0.44 \pm 0.18$
3C 324	RG	1.21	$150 \pm 55$	$37 \pm 30$	$1.0 \pm 0.4$	$0.34 \pm 0.16$	$0.33 \pm 0.28$	$0.34 \pm 0.15$
3C 437	RG	1.48	$710 \pm 180$	$24 \pm 22$	$1.2 \pm 0.5$	$0.91 \pm 0.42$	$1.1 \pm 1.0$	$0.62 \pm 0.28$
3C 68.2	RG	1.575	$210 \pm 70$	$35 \pm 32$	$1.0 \pm 0.5$	$0.41 \pm 0.20$	$0.41 \pm 0.38$	$0.38 \pm 0.18$
3C 322	RG	1.681	$510 \pm 140$	$32 \pm 30$	$1.1 \pm 0.5$	$0.66 \pm 0.33$	$0.68 \pm 0.65$	$0.49 \pm 0.24$
3C 239	RG	1.79	$480 \pm 170$	$37 \pm 36$	$1.0 \pm 0.5$	$0.60 \pm 0.31$	$0.58 \pm 0.57$	$0.45 \pm 0.22$
3C 334	RLQ	0.555	$62 \pm 15$	$50 \pm 46$	$0.8 \pm 0.4$	$0.19 \pm 0.09$	$0.15 \pm 0.14$	$0.23 \pm 0.11$
3C 275.1	RLQ	0.557	$8.8 \pm 2.6$	$2.0 \pm 1.8$	$4.2 \pm 1.9$	$0.35 \pm 0.17$	$1.4 \pm 1.3$	$0.72 \pm 0.33$
3C 254	RLQ	0.734	$63 \pm 20$	$20 \pm 19$	$1.3 \pm 0.6$	$0.30 \pm 0.15$	$0.39 \pm 0.37$	$0.37 \pm 0.18$
3C 175	RLQ	0.768	$130 \pm 30$	$79 \pm 73$	$0.67 \pm 0.31$	$0.21 \pm 0.1$	$0.14 \pm 0.13$	$0.22 \pm 0.10$
3C 68.1	RLQ	1.238	$410 \pm 100$	$79 \pm 73$	$0.68 \pm 0.31$	$0.38 \pm 0.18$	$0.25 \pm 0.23$	$0.30 \pm 0.14$
3C 268.4	RLQ	1.4	$830 \pm 420$	$63 \pm 58$	$0.76 \pm 0.35$	$0.60 \pm 0.32$	$0.45 \pm 0.43$	$0.40 \pm 0.19$
3C 270.1	RLQ	1.519	$790 \pm 210$	$10 \pm 9$	$1.9 \pm 0.9$	$1.48 \pm 0.71$	$2.7 \pm 2.5$	$0.99 \pm 0.46$

<sup>a</sup> Total beam powers are the weighted sum of the beam power from each of the two lobes of each source. Input values for each side of each radio galaxy (RG) are obtained from by O’Dea et al. (2009), who used the data sets of Leahy, Muxlow, & Stephens (1989), Liu, Pooley, & Riley (1992), Guerra, Daly, & Wan (2000), and new observations. The beam power is obtained by applying the equations of strong shock physics to the source. Input values for radio loud quasars (RLQ) are obtained from the compilations of Wellman, Daly, & Wan (1997) and Wan, Daly, & Guerra (2000) after converting quantities to the cosmological model adopted here; the data used for the study originated in the observations of Leahy, Muxlow, & Stephens (1989) and Liu, Pooley, & Riley (1992). Only sources with black hole mass estimates are included.

<sup>b</sup> The value for 3C 405 (Cygnus A) is obtained from Tadhunter et al. (2003); values for the next four sources are obtained from McLure et al. (2004); values for the remaining 14 RG are obtained from McLure et al. (2006). Values for the RLQ are obtained from McLure et al. (2006).

**Table 2.** Black Hole Spins of Sources in Galaxy Clusters

Source (1)	type <sup>a</sup> (2)	z (3)	$L_{44}$ <sup>b</sup> (4)	$M_8$ <sup>c</sup> (5)	$B_{EDD,4}$ (6)	$j_M(B = B_{EDD})$ (7)	$j_M(B = 10^4 G)$ (8)	$j_M(B \propto j)$ (9)
M84	CD	0.0035	$0.01 \pm 0.01$	$3.4 \pm 0.9$	$3.2 \pm 0.4$	$0.009 \pm 0.005$	$0.028 \pm 0.017$	$0.10 \pm 0.03$
M87	CD	0.0042	$0.06 \pm 0.03$	$8.6 \pm 2.9$	$2.0 \pm 0.3$	$0.014 \pm 0.004$	$0.028 \pm 0.011$	$0.10 \pm 0.02$
Centaurus	CD	0.011	$0.074 \pm 0.04$	$8.6 \pm 2.9$	$2.0 \pm 0.3$	$0.015 \pm 0.005$	$0.031 \pm 0.013$	$0.10 \pm 0.02$
HCG 62	CD	0.014	$0.039 \pm 0.04$	$5.7 \pm 2.9$	$2.5 \pm 0.6$	$0.014 \pm 0.008$	$0.034 \pm 0.025$	$0.11 \pm 0.04$
A262	CD	0.016	$0.097 \pm 0.05$	$8.6 \pm 2.9$	$2.0 \pm 0.3$	$0.018 \pm 0.005$	$0.035 \pm 0.015$	$0.11 \pm 0.02$
Perseus	CD	0.018	$1.5 \pm 0.7$	$17 \pm 7$	$1.4 \pm 0.3$	$0.049 \pm 0.015$	$0.070 \pm 0.033$	$0.16 \pm 0.04$
PKS 1404-267	CD	0.022	$0.20 \pm 0.18$	$5.7 \pm 2.9$	$2.5 \pm 0.6$	$0.031 \pm 0.016$	$0.076 \pm 0.051$	$0.16 \pm 0.05$
A2199	CD	0.03	$2.7 \pm 1.6$	$20 \pm 9$	$1.3 \pm 0.3$	$0.061 \pm 0.022$	$0.080 \pm 0.041$	$0.17 \pm 0.04$
A2052	CD	0.035	$1.5 \pm 1.4$	$17 \pm 7$	$1.4 \pm 0.3$	$0.049 \pm 0.024$	$0.070 \pm 0.043$	$0.16 \pm 0.05$
2A 0335+096	CD	0.035	$0.24 \pm 0.15$	$14 \pm 7$	$1.6 \pm 0.4$	$0.022 \pm 0.008$	$0.033 \pm 0.020$	$0.11 \pm 0.03$
MKW 3S	CD	0.045	$4.1 \pm 2.3$	$8.6 \pm 2.9$	$2.0 \pm 0.3$	$0.12 \pm 0.04$	$0.23 \pm 0.10$	$0.29 \pm 0.06$
A4059	CD	0.048	$0.96 \pm 0.62$	$29 \pm 14$	$1.1 \pm 0.3$	$0.031 \pm 0.012$	$0.033 \pm 0.020$	$0.11 \pm 0.03$
Hydra A	CD	0.055	$4.3 \pm 1.3$	$11 \pm 4$	$1.8 \pm 0.3$	$0.10 \pm 0.02$	$0.18 \pm 0.07$	$0.25 \pm 0.05$
A85	CD	0.055	$0.37 \pm 0.24$	$29 \pm 14$	$1.1 \pm 0.3$	$0.019 \pm 0.008$	$0.021 \pm 0.012$	$0.086 \pm 0.026$
Cygnus A	CD	0.056	$13 \pm 7$	$29 \pm 14$	$1.1 \pm 0.3$	$0.11 \pm 0.04$	$0.12 \pm 0.07$	$0.21 \pm 0.06$
Sersic 159/03	CD	0.058	$7.8 \pm 5.4$	$17 \pm 9$	$1.4 \pm 0.4$	$0.11 \pm 0.05$	$0.16 \pm 0.10$	$0.24 \pm 0.07$
A133	CD	0.06	$6.2 \pm 1.4$	$20 \pm 10$	$1.3 \pm 0.3$	$0.093 \pm 0.025$	$0.12 \pm 0.06$	$0.21 \pm 0.05$
A1795	CD	0.063	$1.6 \pm 1.4$	$23 \pm 11$	$1.3 \pm 0.3$	$0.044 \pm 0.022$	$0.054 \pm 0.036$	$0.14 \pm 0.05$
A2029	CD	0.077	$0.87 \pm 0.27$	$60 \pm 36$	$0.77 \pm 0.23$	$0.020 \pm 0.007$	$0.015 \pm 0.009$	$0.073 \pm 0.023$
A478	CD	0.081	$1.0 \pm 0.5$	$26 \pm 14$	$1.2 \pm 0.3$	$0.033 \pm 0.012$	$0.038 \pm 0.023$	$0.12 \pm 0.04$
A2597	CD	0.085	$0.67 \pm 0.58$	$8.6 \pm 2.9$	$2.0 \pm 0.3$	$0.047 \pm 0.022$	$0.093 \pm 0.051$	$0.18 \pm 0.05$
3C 388	CD	0.092	$2.0 \pm 1.8$	$17 \pm 7$	$1.4 \pm 0.3$	$0.057 \pm 0.028$	$0.081 \pm 0.049$	$0.17 \pm 0.05$
PKS 0745-191	CD	0.103	$17 \pm 9$	$31 \pm 16$	$1.1 \pm 0.3$	$0.12 \pm 0.04$	$0.13 \pm 0.07$	$0.21 \pm 0.06$
Hercules A	CD	0.154	$3.1 \pm 2.5$	$20 \pm 11$	$1.3 \pm 0.4$	$0.066 \pm 0.032$	$0.086 \pm 0.060$	$0.17 \pm 0.06$
Zw 2701	CD	0.214	$60 \pm 62$	$17 \pm 9$	$1.4 \pm 0.4$	$0.31 \pm 0.18$	$0.44 \pm 0.32$	$0.40 \pm 0.14$
MS 0735.6+7421	CD	0.216	$69 \pm 51$	$20 \pm 11$	$1.3 \pm 0.4$	$0.31 \pm 0.14$	$0.41 \pm 0.28$	$0.38 \pm 0.13$
4C 55.16	CD	0.242	$4.2 \pm 3.0$	$14 \pm 7$	$1.6 \pm 0.4$	$0.09 \pm 0.039$	$0.14 \pm 0.09$	$0.22 \pm 0.07$
A1835	CD	0.253	$18 \pm 13$	$54 \pm 36$	$0.81 \pm 0.27$	$0.10 \pm 0.05$	$0.076 \pm 0.057$	$0.16 \pm 0.06$
Zw 3146	CD	0.291	$58 \pm 42$	$74 \pm 53$	$0.70 \pm 0.25$	$0.15 \pm 0.07$	$0.10 \pm 0.08$	$0.19 \pm 0.08$

<sup>a</sup> Almost all of the sources have FRI or amorphous radio structure except for a few exceptions such as Cygnus A (Birzan et al. 2008).

<sup>b</sup> Beam powers are obtained from Rafferty et al. (2006) who combine the total cavity pressure and volume with the buoyancy timescale to determine the beam power.

<sup>c</sup> Black hole masses are obtained from the values  $M_{BH,LK}$  listed in Table 3 of Rafferty et al. (2006) after removing the 0.35 correction factor introduced in that paper. This brings the black hole mass estimates of Cygnus A (3C 405) and M84 into reasonably good agreement with the independent determinations of Tadhunter et al. (2003) and Maciejewski & Binney (2001), respectively.

**Table 3.** FRII Black Hole Spin Energy and Fraction of Spin Energy Extracted

Source (1)	type (2)	$\frac{E_*}{Mc^2} (10^{-3})^a$ (3)	$\frac{E_s(B=B_{EDD})}{Mc^2}$ (4)	$f(B = B_{EDD})$ (5)	$\frac{E_s(B=10^4G)}{Mc^2}$ (6)	$f(B = 10^4G)$ (7)
3C 405	RG	1.3 ± 0.4	0.0067 ± 0.0022	0.195 ± 0.016	0.0092 ± 0.0055	0.141 ± 0.041
3C 244.1	RG	1.9 ± 1.4	0.0050 ± 0.0037	0.379 ± 0.050	0.019 ± 0.027	0.102 ± 0.072
3C 172	RG	3.6 ± 2.6	0.014 ± 0.011	0.253 ± 0.033	0.07 ± 0.13	0.049 ± 0.034
3C 330	RG	3.3 ± 2.4	0.023 ± 0.018	0.145 ± 0.019	0.07 ± 0.12	0.049 ± 0.034
3C 427.1	RG	1.8 ± 1.3	0.0077 ± 0.0057	0.235 ± 0.029	0.019 ± 0.027	0.096 ± 0.067
3C 337	RG	2.5 ± 1.8	0.0079 ± 0.0059	0.316 ± 0.043	0.032 ± 0.048	0.079 ± 0.055
3C34	RG	2.4 ± 1.7	0.014 ± 0.011	0.168 ± 0.012	0.031 ± 0.048	0.077 ± 0.054
3C441	RG	2.3 ± 1.7	0.013 ± 0.010	0.173 ± 0.015	0.027 ± 0.041	0.086 ± 0.061
3C 55	RG	4.3 ± 3.2	0.048 ± 0.042	0.089 ± 0.012	0.16 ± 0.44	0.027 ± 0.020
3C 247	RG	1.2 ± 0.9	0.0047 ± 0.0037	0.253 ± 0.034	0.0063 ± 0.0094	0.19 ± 0.14
3C 289	RG	1.6 ± 1.3	0.0113 ± 0.0094	0.141 ± 0.016	0.015 ± 0.024	0.109 ± 0.085
3C 280	RG	1.3 ± 1.1	0.0070 ± 0.0059	0.186 ± 0.026	0.009 ± 0.014	0.15 ± 0.12
3C 356	RG	2.7 ± 2.3	0.034 ± 0.033	0.079 ± 0.013	0.042 ± 0.078	0.064 ± 0.052
3C 267	RG	2.6 ± 2.2	0.029 ± 0.027	0.089 ± 0.012	0.042 ± 0.078	0.062 ± 0.051
3C 324	RG	1.6 ± 1.4	0.015 ± 0.014	0.105 ± 0.019	0.014 ± 0.024	0.116 ± 0.099
3C 437	RG	5.5 ± 5.1	0.16 ± 0.27	0.0350 ± 0.0045	—	—
3C 68.2	RG	2 ± 1.9	0.022 ± 0.023	0.091 ± 0.015	0.022 ± 0.043	0.091 ± 0.085
3C 322	RG	3.3 ± 3.2	0.065 ± 0.077	0.0510 ± 0.0072	0.07 ± 0.16	0.047 ± 0.045
3C 239	RG	2.8 ± 2.8	0.052 ± 0.062	0.054 ± 0.010	0.05 ± 0.11	0.060 ± 0.059
3C 270.1	RLQ	13.1 ± 7.7	—	—	—	—
3C 268.4	RLQ	2.1 ± 1.3	0.052 ± 0.064	0.041 ± 0.010	0.027 ± 0.055	0.080 ± 0.050
3C 68.1	RLQ	1.33 ± 0.78	0.019 ± 0.019	0.0710 ± 0.0090	0.008 ± 0.015	0.167 ± 0.098
3C 175	RLQ	0.71 ± 0.41	0.0057 ± 0.0055	0.125 ± 0.012	0.0025 ± 0.0046	0.29 ± 0.17
3C 254	RLQ	1.9 ± 1.1	0.011 ± 0.012	0.164 ± 0.025	0.020 ± 0.040	0.094 ± 0.056
3C 275.1	RLQ	7.7 ± 4.6	0.016 ± 0.016	0.488 ± 0.071	—	—
3C 334	RLQ	0.73 ± 0.43	0.0044 ± 0.0042	0.168 ± 0.020	0.0030 ± 0.0056	0.25 ± 0.15

<sup>a</sup> The total outflow energy  $E_*$  is taken to be the weighted sum of the outflow energy of each side of a source; the values for the RG were obtained from Daly (2009a) who used the outflow energies listed by O’Dea et al. (2009) for the radio galaxies; values for RLQ were obtained in an identical manner.

**Table 4.** CD Black Hole Spin Energy and Fraction of Spin Energy Extracted

Source (1)	$\frac{E_*}{Mc^2}(10^{-3})^a$ (2)	$\frac{E_s(B=B_{EDD})}{Mc^2}$ (3)	$f(B = B_{EDD})$ (4)	$\frac{E_s(B=10^4G)}{Mc^2}$ (5)	$f(B = 10^4G)$ (6)
M84	0.00019 ± 0.00023	0.000010 ± 0.000011	0.019 ± 0.022	0.00010 ± 0.00012	0.0020 ± 0.0024
M87	0.00052 ± 0.00028	0.000024 ± 0.000013	0.0210 ± 0.0089	0.000097 ± 0.000077	0.0050 ± 0.0017
Centaurus	0.0016 ± 0.0010	0.000030 ± 0.000018	0.052 ± 0.029	0.00012 ± 0.00010	0.0130 ± 0.0035
HCG 62	0.0018 ± 0.0022	0.000024 ± 0.000028	0.075 ± 0.082	0.00014 ± 0.00021	0.0130 ± 0.0059
A262	0.0034 ± 0.0020	0.000039 ± 0.000024	0.086 ± 0.012	0.00016 ± 0.00013	0.0210 ± 0.0076
Perseus	0.25 ± 0.19	0.00030 ± 0.00018	0.81 ± 0.53	0.00061 ± 0.00057	0.41 ± 0.32
PKS 1404-267	0.0047 ± 0.0045	0.00012 ± 0.00012	0.038 ± 0.010	0.00073 ± 0.00097	0.0060 ± 0.0034
A2199	0.083 ± 0.057	0.00047 ± 0.00034	0.178 ± 0.035	0.00081 ± 0.00083	0.103 ± 0.049
A2052	0.022 ± 0.022	0.00030 ± 0.00030	0.072 ± 0.013	0.00061 ± 0.00075	0.036 ± 0.016
2A 0335+096	0.017 ± 0.013	0.000058 ± 0.000046	0.293 ± 0.037	0.00014 ± 0.00016	0.122 ± 0.063
MKW 3S	0.99 ± 0.65	0.0017 ± 0.0011	0.591 ± 0.005	0.0068 ± 0.0060	0.146 ± 0.049
A4059	0.023 ± 0.018	0.00012 ± 0.00010	0.200 ± 0.062	0.00014 ± 0.00017	0.167 ± 0.098
Hydra A	1.24 ± 0.74	0.00131 ± 0.00062	0.95 ± 0.44	0.0040 ± 0.0032	0.314 ± 0.035
A85	0.0093 ± 0.0078	0.000045 ± 0.000037	0.21 ± 0.14	0.000054 ± 0.000064	0.173 ± 0.082
Cygnus A	0.65 ± 0.46	0.0016 ± 0.0011	0.412 ± 0.010	0.0019 ± 0.0021	0.34 ± 0.17
Sersic 159/03	0.32 ± 0.27	0.0016 ± 0.0014	0.204 ± 0.027	0.0032 ± 0.0039	0.102 ± 0.053
A133	0.27 ± 0.15	0.00108 ± 0.00059	0.247 ± 0.062	0.0019 ± 0.0019	0.144 ± 0.070
A1795	0.046 ± 0.046	0.00024 ± 0.00025	0.188 ± 0.013	0.00037 ± 0.00049	0.125 ± 0.063
A2029	0.018 ± 0.012	0.000050 ± 0.000034	0.353 ± 0.031	0.000029 ± 0.000035	0.62 ± 0.37
A478	0.013 ± 0.010	0.00014 ± 0.00010	0.096 ± 0.048	0.00018 ± 0.00022	0.072 ± 0.040
A2597	0.093 ± 0.085	0.00027 ± 0.00025	0.344 ± 0.061	0.0011 ± 0.0012	0.086 ± 0.033
3C 388	0.067 ± 0.068	0.00041 ± 0.00040	0.17 ± 0.15	0.0008 ± 0.0010	0.083 ± 0.030
PKS 0745-191	0.49 ± 0.34	0.0019 ± 0.0013	0.259 ± 0.038	0.0021 ± 0.0023	0.24 ± 0.12
Hercules A	0.34 ± 0.34	0.00054 ± 0.00053	0.639 ± 0.010	0.0009 ± 0.0013	0.37 ± 0.21
Zw 2701	4.5 ± 5.2	0.013 ± 0.015	0.36 ± 0.38	0.026 ± 0.040	0.175 ± 0.084
MS 0735.6+7421	18 ± 16	0.012 ± 0.012	1.44 ± 0.25	0.022 ± 0.031	0.82 ± 0.49
4C 55.16	0.19 ± 0.16	0.00102 ± 0.00089	0.182 ± 0.047	0.0025 ± 0.0030	0.076 ± 0.043
A1835	0.19 ± 0.19	0.0012 ± 0.0011	0.17 ± 0.12	0.0007 ± 0.0011	0.26 ± 0.17
Zw 3146	1.1 ± 1.2	0.0027 ± 0.0028	0.42 ± 0.31	0.0013 ± 0.0020	0.91 ± 0.61

<sup>a</sup> The total energy is obtained from Rafferty et al. (2006).